THE JOURNAL OF BIOLOGICAL CHEMISTRY
Vol. 277, No. 42, Issue of October 18, pp. 39722–39727, 2002

Printed in U.S.A.

Carbamoyl-phosphate Synthetase

CREATION OF AN ESCAPE ROUTE FOR AMMONIA*

Received for publication, July 10, 2002
Published, JBC Papers in Press, July 18, 2002, DOI 10.1074/jbc.M206915200

James B. Thoden‡, Xinyi Huang§¶, Frank M. Raushel§‖, and Hazel M. Holden‡**

From the ‡Department of Biochemistry, University of Wisconsin, Madison, Wisconsin, 53706-1544 and the §Department of Chemistry, Texas A&M University, College Station, Texas 77843-3012

Carbamoyl-phosphate synthetase catalyzes the production of carbamoyl phosphate through a reaction mechanism requiring one molecule of bicarbonate, two molecules of MgATP, and one molecule of glutamine. The enzyme from *Escherichia coli* is composed of two polypeptide chains. The smaller of these belongs to the Class I amidotransferase superfamily and contains all of the necessary amino acid side chains required for the hydrolysis of glutamine to glutamate and ammonia. Two homologous domains from the larger subunit adopt conformations that are characteristic for members of the ATP-grasp superfamily. Each of these ATP-grasp domains contains an active site responsible for binding one molecule of MgATP. High resolution x-ray crystallographic analyses have shown that, remarkably, the three active sites in the *E. coli* enzyme are connected by a molecular tunnel of ~100 Å in total length. Here we describe the high resolution x-ray crystallographic structure of the G359F (small subunit) mutant protein of carbamoyl phosphate synthetase. This residue was initially targeted for study because it resides within the interior wall of the molecular tunnel leading from the active site of the small subunit to the first active site of the large subunit. It was anticipated that a mutation to the larger residue would "clog" the ammonia tunnel and impede the delivery of ammonia from its site of production to the site of utilization. In fact, the G359F substitution resulted in a complete change in the conformation of the loop delineated by Glu-355 to Ala-364, thereby providing an "escape" route for the ammonia intermediate directly to the bulk solvent. The substitution also effected the disposition of several key catalytic amino acid side chains in the small subunit active site.

The concept of substrate channeling, as described in Ref. 1, was originally put forth to explain the manner in which reactive intermediates are transferred from one protein to another in a metabolic pathway or shuttled from one active site to another within a single enzyme. Many have regarded this phenomenon as an essential mechanism for the regulation of metabolic pathways within the living cell. Obvious advantages of substrate channeling include the protection of unstable intermediates or products, the sequestering of toxic molecules, the control of metabolic flux, the improvement of catalytic efficiency, and the decreased diffusion of substrates or intermediates away from their respective active sites. Recent reviews on the topic of substrate channeling can be found in Refs. 2–4.

While substrate channeling is now a widely accepted concept, there is still a paucity of mechanistic and structural data pertaining to this complex biological phenomenon, although this situation is changing rapidly. The first direct structural observation for substrate channeling was derived from the elegant x-ray crystallographic analysis of tryptophan synthase isolated from *Salmonella typhimurium* (5). This investigation demonstrated that the two active sites located on the α- and β-subunits of the enzyme were separated by a distance of ~25 Å and connected by a tunnel of the appropriate diameter to facilitate the diffusion of indole. As more complicated protein structures are solved to increasingly higher resolution, it is becoming apparent that substrate channels and tunnels may, indeed, be quite common. Since the initial x-ray analysis of tryptophan synthase other examples of enzymes employing substrate channeling have appeared in the literature including carbamoyl-phosphate synthetase (6), GMP synthetase (7), glutamine phosphoribosylpyrophosphate amidotransferase (8), asparagine synthetase (9), and glucosamine-6-phosphate synthase (10), among others.

Carbamoyl-phosphate synthetase (CPS),[1] the focus of this report, catalyzes the production of carbamoyl phosphate, which is subsequently employed in both pyrimidine and arginine biosynthesis in eukaryotes and prokaryotes. The enzyme from *Escherichia coli* has been the subject of extensive biochemical analysis for well over thirty years due, in part, to its interesting catalytic mechanism. Recent reviews of the enzyme can be found in Refs. 11–13. As shown in Scheme 1, CPS synthesizes carbamoyl phosphate from two molecules of MgATP, one molecule of bicarbonate, and one molecule of glutamine using a catalytic mechanism that proceeds through three reactive intermediates: carboxy phosphate, ammonia, and carbamate.

As isolated from *E. coli*, CPS is an α,β-heterodimeric protein with the individual large and small subunits containing 1073 and 382 amino acid residues, respectively (14, 15). The smaller

* This research was supported in part by National Institutes of Health Grants GM55513 (to H. M. H.) and DK30343 (to F. M. R.) and the Robert A. Welch Foundation Grant A840. Use of the Argonne National Laboratory Structural Biology Center beamlines at the Advanced Photon Source was supported by the United States Department of Energy, Office of Energy Research under contract no. W-31-109-ENG-38. The costs of publication of this article were defrayed in part by the payment of page charges. This article must therefore be hereby marked "*advertisement*" in accordance with 18 U.S.C. Section 1734 solely to indicate this fact.

The atomic coordinates and structure factors (code 1M6V) have been deposited in the Protein Data Bank, Research Collaboratory for Structural Bioinformatics, Rutgers University, New Brunswick, NJ (http://www.rcsb.org/).

¶ Present address: Wyeth Research, Dept. of Biological Chemistry, 401 N. Middleton Rd., Pearl River, NY 10923.

‖ To whom correspondence may be addressed. Tel.: 979-845-3373; Fax: 979-845-9452; E-mail: Raushel@tamu.edu.

** To whom correspondence may be addressed. Tel.: 608-262-4988; Fax: 608-262-1319; E-mail: Hazel_Holden@biochem.wisc.edu.

[1] The abbreviation used is: CPS, carbamoyl-phosphate synthetase.

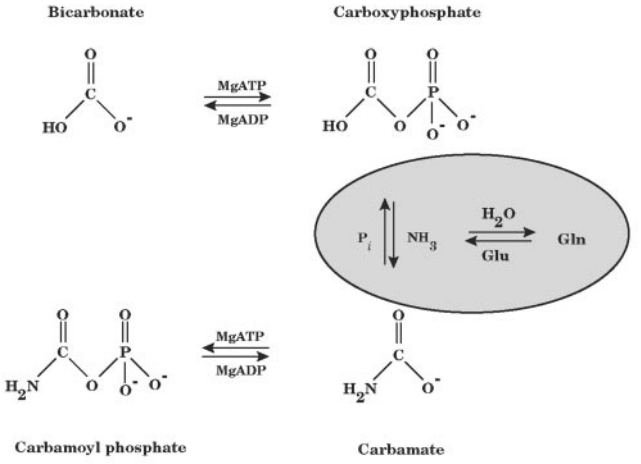

SCHEME 1

subunit catalyzes the hydrolysis of glutamine to glutamate and ammonia and belongs to the Class I amidotransferase superfamily (16), whereas the larger subunit harbors the binding sites for both molecules of MgATP, allosteric ligands such as UMP and ornithine, and various metal ions. This larger subunit, indeed, contains all of the necessary hardware to produce carbamoyl phosphate with only ammonia as the nitrogen source (17).

The recent x-ray crystallographic studies of CPS from *E. coli* have shed considerable light on this remarkable molecular machine. As shown in Fig. 1, and quite unexpectedly, the three active sites of the enzyme are widely spaced throughout the α,β-heterodimer (6, 18–22). By both visual inspection of the CPS model and the employment of computational searches with the software package GRASP (23), it was possible to map out a molecular tunnel connecting the three active sites as indicated in Fig. 1. Accordingly, the ammonia generated by the small subunit traverses the molecular tunnel leading to the binding site for the first molecule of MgATP where it reacts with the carboxy phosphate intermediate to generate carbamate. This particular region has been referred to as the "ammonia" tunnel and is built from amino acid residues contributed by both the small subunit and the N-terminal half of the large subunit. Similarly, the carbamate shuttles between the first and second MgATP binding sites in the large subunit in a channel referred to as the carbamate tunnel to generate the final product, carbamoy phosphate.

To test the validity of the molecular tunnel mapped out in the CPS structure, a series of site-directed mutant proteins were created within the ammonia tunnel and kinetically studied (24, 25). One position in particular was targeted for analysis, namely Gly-359 of the small subunit, which forms an integral part of the interior wall of the putative molecular tunnel. These investigations demonstrated a direct correlation between the size of the substituted amino acid and the extent of the uncoupling of the partial reactions catalyzed by CPS, specifically glutamine and MgATP hydrolysis. The simplest explanation for these results was the formation of a blockage within the tunnel such that ammonia could no longer diffuse from the small subunit to the first active site of the large subunit. Here we describe the high resolution structure of one of these mutant proteins, namely the G359F enzyme. Rather than cause a blockage of the tunnel, the mutation resulted in the formation of an escape route for ammonia through a path leading directly to the bulk solvent. The implication of this, with respect to the evolution of substrate tunnels, is discussed.

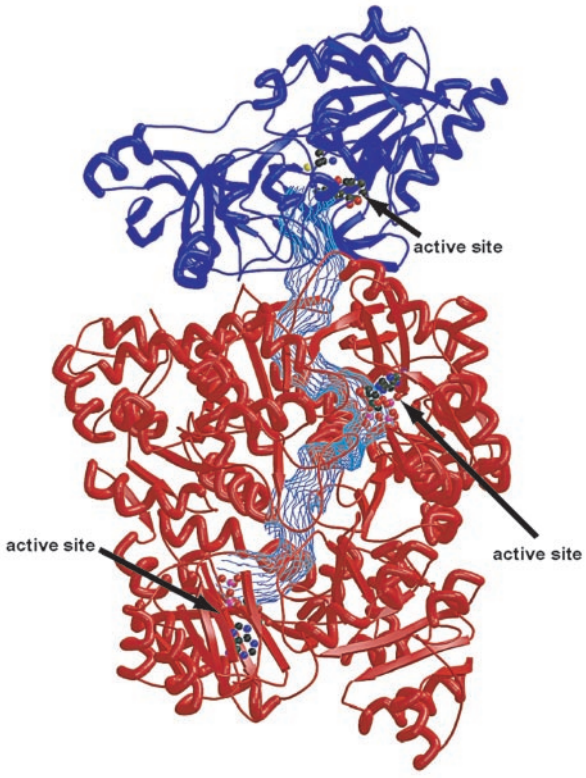

FIG. 1. **Ribbon representation of one α,β-heterodimer of CPS.** The small subunit of CPS is displayed in *blue*, whereas the large subunit is depicted in *red*. The molecular conduit connecting the three active sites is shown in a chicken wire representation. All figures were prepared with the software package MOLSCRIPT (34).

TABLE I
Relevant x-ray data collection statistics

Resolution	Independent reflections	Completeness	Redundancy	Avg I/Avg (I)	R_{sym}[a]
(Å)		(%)			
30.0–2.10	445772	92.1	3.5	16.2	7.6
2.18–2.10[b]	40543	84.4	2.5	2.7	24.4

[a] $R_{sym} = (\Sigma|\ I - \bar{I}\ |/\ \Sigma\ I) \times 100$.
[b] Statistics for the highest resolution bin.

EXPERIMENTAL PROCEDURES

Crystallization Procedures—Protein samples employed for crystallization trials were purified as previously described (26). Large single crystals were grown at 4 °C by batch from 8% polyethylene glycol 8000, 0.65 M tetraethylammonium chloride, 0.5 mM $MnCl_2$, 100 mM KCl, 1.5 mM ADP, 0.5 mM L-ornithine, and 25 mM HEPPS (pH 7.4). Once the crystals reached dimensions of ~0.3 mm × 0.3 mm × 0.8 mm, they were flash-frozen according to previously published procedures (6) and stored under liquid nitrogen until synchrotron beam time became available. The crystals belonged to the space group $P2_12_12_1$ with unit cell dimensions of a = 151.1 Å, b = 164.2 Å, and c = 331.5 Å and one complete $(\alpha,\beta)_4$-heterotetramer per asymmetric unit.

X-ray Data Collection and Processing—An x-ray data set for the G359F mutant protein was collected on a 3 × 3-tiled "SBC2" charge-coupled device detector at the Structural Biology Center 19-ID Beamline (Advanced Photon Source, Argonne National Laboratory). The data were processed with HKL2000 and scaled with SCALEPACK (27). Relevant data collection statistics are presented in Table I.

The structure of the G359F mutant protein was solved by Difference Fourier techniques to a nominal resolution of 2.1 Å. The initial model was subjected to least-squares refinement with the software package TNT (28), which reduced the overall R-factor to 26.8%. With more than 5800 amino acid residues in the asymmetric unit, the goal of the subsequent model building process was to lower the R-factor as much as possible using an "averaged" α,β-heterodimer before finally rebuilding the entire $(\alpha,\beta)_4$-heterotetramer in the asymmetric unit. Thus, to expe-

dite the structure refinement process, the electron densities corresponding to the four α,β-heterodimers in the asymmetric unit were averaged with the program AVE in the RAVE suite of programs and the averaged model adjusted according to the map (29, 30). This averaging and rebuilding process lowered the overall R-factor to 21.0%. Next the averaged model was used to create the entire $(\alpha,\beta)_4$-heterotetramer, which was placed back into the unit cell. Maps were calculated with coefficients of the form $(2F_o - F_c)$, where F_o was the native structure factor amplitude and F_c was the calculated structure factor amplitude from the model, and the four α,β-heterodimers in the asymmetric unit were adjusted to the electron density using the program TURBO (31). The final R-factor was 18.0% for all measured x-ray data. Relevant refinement statistics are given in Table II. For the sake of simplicity, the following discussion refers only to the third α,β-heterodimer in the x-ray coordinate file deposited in the Research Collaboratory for Structural Bioinformatics.

RESULTS AND DISCUSSION

Previous studies have demonstrated that the G359F mutation within the small subunit of CPS results in substantial changes in specific kinetic constants for the modified protein relative to those for the wild-type enzyme. For example, in the partial reaction for the hydrolysis of glutamine (in the absence of ATP), k_{cat} is bigger for the mutant protein than for the wild-type enzyme by about one order of magnitude. However, the K_m of glutamine for this reaction is increased by a factor $>$ 400, relative to the wild-type enzyme. Nevertheless, in the presence of ATP/bicarbonate, the maximal rate of glutamine hydrolysis for the mutant protein is essentially the same as for the wild-type enzyme, although the K_m for glutamine remains high. These results demonstrate that the catalytic machinery of the G359F mutant protein for the hydrolysis of glutamine is intact and that the enhancement in the rate of glutamine hydrolysis, allosterically induced through the formation of carboxy phosphate within the large subunit of CPS, is fully operational. What has significantly changed with this mutation is the apparent binding affinity for the association of glutamine to the active site within the small subunit.

For the bicarbonate-dependent ATP hydrolysis reaction (in the absence of glutamine) there is a 6-fold increase in the value of k_{cat} for the mutant relative to the wild-type protein. However, there is essentially no increase in the rate of ATP hydrolysis for the G359F mutant protein in the presence of saturating levels of glutamine. The enhanced rate for the partial ATPase reaction (in the absence of glutamine) with the mutant protein is consistent with a greater instability of the carboxy phosphate intermediate apparently due to greater access by solvent water. The abolition of the rate enhancement for ATP turnover in the presence of glutamine for the mutant protein is fully consistent with the impedance of ammonia during delivery to the large subunit. This conclusion is also supported by the diminished rate of synthesis of carbamoyl phosphate while employing glutamine as the nitrogen source. With the mutant protein, the value of k_{cat}/K_m for carbamoyl-phosphate synthesis is reduced by 13,000-fold relative to that of the wild-type protein (24) and the overall value of k_{cat} is reduced by a factor of ~60. However, the rate of carbamoyl phosphate formation using ammonia as a nitrogen source is essentially unchanged from the value observed with the wild-type enzyme. Thus, the G359F mutation results in both a significant increase in the K_m for glutamine and in the inability of the enzyme to make carbamoyl phosphate using glutamine (but not ammonia) as a

TABLE II
Relevant least-squares refinement statistics

Resolution limits (Å)	30.0–2.1
[a]R-factor (overall) %/no. reflections	18.0/440901
R-factor (working) %/no. reflections	17.4/396875
R-factor (free) %/no.rflns	24.5/44026
[b]No. protein atoms	44271
[c]No. Hetero-atoms	3935
Weighted root mean square deviations from ideality	
Bond lengths (Å)	0.012
Bond angles (degrees)	2.33
Trigonal planes (Å)	0.006
General planes (Å)	0.012
[d]Torsional angles (degrees)	17.7

[a] R-factor = $(\Sigma \mid F_o - F_c \mid / \Sigma \mid F_o \mid) \times 100$ where F_o is the observed structure-factor amplitude and F_c is the calculated structure-factor.

[b] These include multiple conformations for the following: Heterodimer 1: Ser-29, Glu-59, Lys-104, Asp-518, Glu-676, and Met-772 in the large subunit and Lys-257 in the small subunit: heterodimer 2: Thr-5, Arg-149, Lys-423, Arg-1004, and Thr-1017 in the large subunit and Arg-50 and Asn-232 in the small subunit; heterodimer 3: Lys-8, Ser-29, Glu-278, Met-563, Val-773, and Gln-967 in the large subunit and Gln-272, Met-286, and Lys-379 in the small subunit; and heterodimer 4: Glu-153, Leu-415, Asn-554, Gln-645, Gln-814, and Asn-1007 in the large subunit and Lys-230 in the small subunit.

[c] These include: 26 potassium ions, 12 manganese ions, 4 tetraethylammonium ions, 28 choride ions, 8 ADP molecules, 4 L-ornithines, 4 inorganic phosphates, and 3561 water molecules.

[d] The torsional angles were not restrained during the refinement.

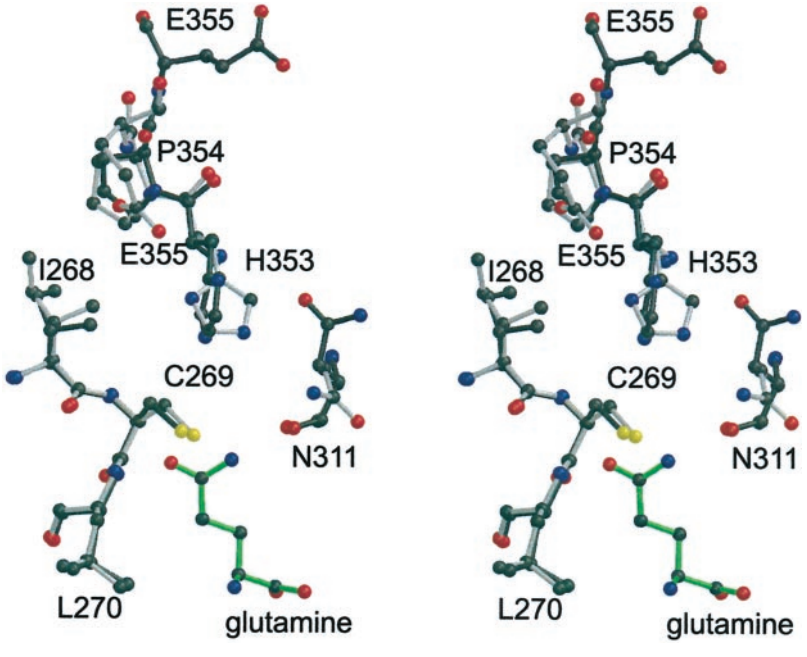

FIG. 2. **Superposition of the small subunit active sites for the wild-type and G359F proteins.** The wild-type enzyme is depicted in *gray* bonds, whereas the G359F mutant protein is drawn in *black* bonds. The position of the glutamine, highlighted in *green* bonds, is based on the structure of the previously solved C269S mutant protein with bound substrate (22). Note the difference in conformations of His-353, Glu-355, and Asn-311 between the two forms of the protein.

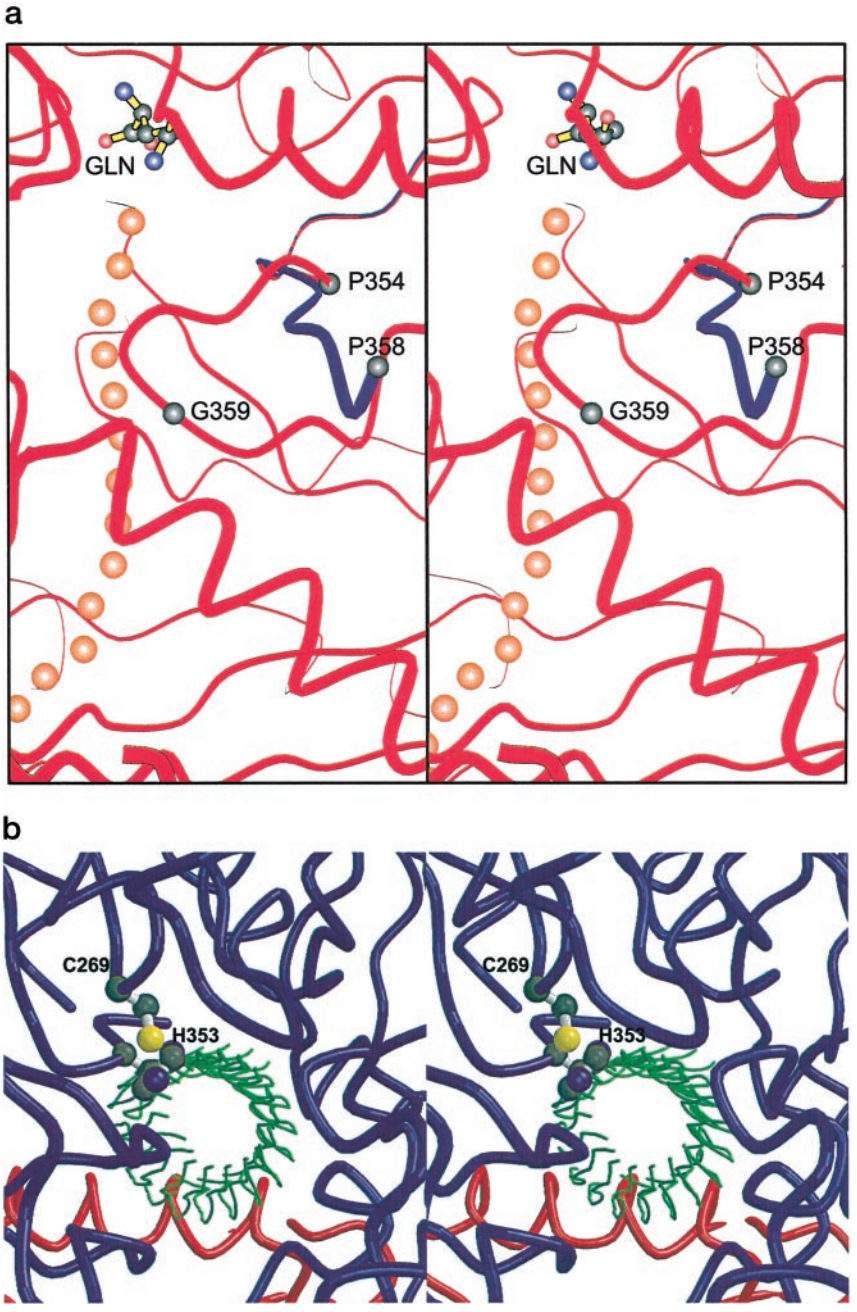

FIG. 3. **The escape route for ammonia.** Shown in *a* is a close-up view of the ammonia tunnel near the site of the mutation. The wild-type enzyme is depicted in *red* with the course of the ammonia tunnel marked by the *orange* spheres. The *blue* ribbon denotes the change in direction of the loop as a result of the G359F mutation. Note that the polypeptide chain for the mutant protein from Phe-359 to Asp-363 is disordered. In *b*, the small and large subunits are color-coded in *blue* and *red*, respectively. The escape route, indicated by the *green* chicken wire representation, was calculated with the program ALIMENTARY (6). In the wild-type enzyme, the loop defined by Gly-359 to Asp-363 passes directly through the escape route, thereby blocking ammonia release. The positions for Cys-269 and His-353, which form the catalytic dyad, are indicated by the ball-and-stick representations.

nitrogen source. The mutant protein can hydrolyze glutamine and can catalyze the formation of the carboxy phosphate intermediate, but it is unable to couple the reactions catalyzed at the individual active sites toward the production of carbamoyl phosphate.

The question as to whether these alterations to the kinetic constants are from major structural perturbations of the protein architecture or rather from a simple blocking of the putative ammonia channel is addressed here by a high resolution x-ray crystallographic analysis. The G359F substitution in the small subunit results in virtually no perturbations in the conformation of the large subunit of the enzyme and, particularly, within the two MgATP binding pockets. Indeed, the α-carbons alone or all atoms comprising the large subunit of the mutant protein superimpose onto the wild-type enzyme with root mean square deviations of 0.25 and 1.20 Å, respectively.

The situation is more complex, however, with regard to the small subunit and to its active site region. The α-carbons alone or all atoms comprising the small subunit of the mutant protein superimpose onto the wild-type enzyme with root mean square deviations of 1.05 and 1.20 Å, respectively. Shown in Fig. 2 is a superposition of the wild-type and G359F mutant proteins near the glutaminase active site of the small subunit. In the wild-type enzyme, as in all Class I amidotransferases examined to date, Cys-269 and His-353 (or their structural equivalents) function as a catalytic couple with His-353 serving to deprotonate the side chain thiol of Cys-269. Additionally, there is a conserved glutamate in the Class I amidotransferases, namely Glu-355 in CPS, which hydrogen bonds to the imidazole group of His-353. In wild-type CPS, $O^{\delta 1}$of Glu-355 lies within 2.9 Å from $N^{\delta 1}$ of His-353. Most likely Glu-355 plays a key role in correctly positioning the side chain of His-353 for effective deprotonation of Cys-269. The mutation of Glu-355 to an alanine residue, however, has no effect on the maximal rate of glutamine hydrolysis but does result in an order of magnitude increase in the K_m for glutamine (32). Upon substituting a glycine with a phenylalanine residue at position 359, the polypeptide chain in the nearby vicinity adopts a quite different conformation as can be seen in

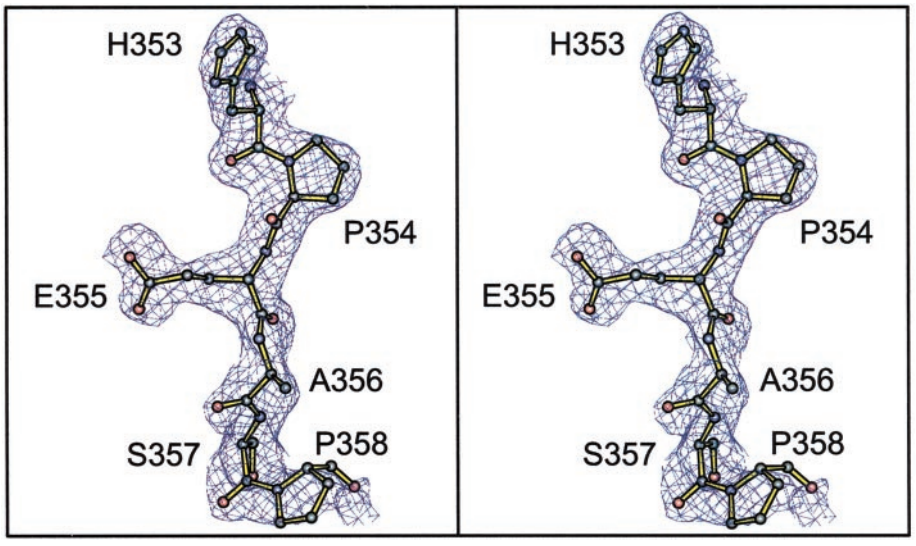

FIG. 4. **Electron density corresponding to the region from His-353 to Ser-357 in the mutant protein.** The map was contoured at 1 σ and calculated with coefficients of the form $(2F_o - F_c)$, where F_o was the native structure factor amplitude and F_c was the calculated structure factor amplitude.

Fig. 2. The net result is that the carboxylate group of Glu-355 is no longer within hydrogen bonding distance to His-353 but rather is positioned at ~8.0 Å away. Additionally, the side chain $O^{\delta 1}$ of Asn-311, which normally hydrogen bonds to $N^{\delta 1}$ of His-291, rotates by ~159 ° and ~60 ° about the Cα/Cβ and Cβ/Cγ bonds, respectively, thereby allowing it to interact with $N^{\delta 1}$ of His-353 (3.2 Å). This distance in wild-type CPS is ~5.5 Å.

The path of the ammonia tunnel in native CPS is outlined in Fig. 3*a*. Gly-359 of the small subunit is positioned within the random coil area delineated by Glu-355 to Ala-364, and it is this region that provides one side of the ammonia tunnel. The goal of the G359F mutation was to block this conduit for the passage of ammonia, and, indeed, the observed kinetics parameters for the G359F mutant protein clearly indicate the importance of this region for communication between active sites and for the ultimate synthesis of carbamoyl phosphate. Unexpectedly, however, the G359F mutation resulted in a change in conformation for this random coil region beginning at Pro-354. Electron density corresponding to this region in the G359F mutant protein is displayed in Fig. 4. Note that the region of the polypeptide chain from Phe-359 (the site of the mutation) to Asp-363 is disordered in the electron density map. In wild-type CPS, Pro-354 adopts torsional angles of $\phi = -70$ ° and $\psi = -21$ °. In the G359F mutant protein, these torsional angles are $\phi = -56$ ° and $\psi = 145$ ° with the net effect of opening up one side of the ammonia tunnel and sending the polypeptide chain off into an extended conformation. The distance between the prolines at position 358 in the two structures is ~13 Å. This change at Pro-354 could not have been predicted given that in the wild-type enzyme the α-carbons for Pro-354 and Gly-359 are separated by ~9 Å. As a result of the changes in the polypeptide chain conformation between Glu-355 and Ala-364, the structural integrity of the ammonia tunnel has been compromised and an accompanying new "escape route" for the ammonia intermediate has been formed as indicated in Fig. 3*b*. This escape route undoubtedly contributes to the uncoupling of the separate chemical reactions in the G359F mutant form of CPS.

One of the more intriguing questions concerning enzymes that employ substrate channeling in their reaction mechanisms is the manner in which these molecular tunnels first evolved. There are examples in the literature, such as CPS and tryptophan synthetase (5), whereby the molecular channels are fully formed even in the absence of a full complement of substrates. In some enzymes, though, it appears as if the channels only exist transiently during each catalytic cycle such as in glutamine phosphoribosylpyrophosphate amidotransferase (8). For those enzymes containing permanent substrate channels, two possible mechanisms for tunnel evolution can be envisioned. In one scenario, smaller amino acid residues are substituted for larger side chains, thereby creating incremental cavities throughout the interior of the protein that eventually merge into a tunnel connecting active sites. The difficulty with this scenario, however, is that the creation of cavities within the interior of a protein has been demonstrated to have, in general, a destabilizing effect (33). Another mechanism of channel formation that can be envisioned involves single point mutations where smaller amino acid residues within the interior of a enzyme are substituted with larger side chains, thereby leading to substantial conformational changes in the protein architecture. Although most of these changes would be disruptive and lead to a loss of proper folding or catalytic activity, it would be expected that some could give rise to the formation of new tunnels. This second scenario seems more likely since, as demonstrated in this investigation, single point mutations can have profound effects on the polypeptide chain conformation far from the original site of the substitution.

In summary, as has been so often the case in other protein site-directed mutagenesis studies, the replacement of a single amino acid in the ammonia tunnel of CPS resulted in changes in its three-dimensional architecture that could not have been anticipated. Rather than "clog" the ammonia tunnel, the G359F mutation resulted both in the formation of a new pathway for ammonia dispersion and in altered conformations of key catalytic residues within the glutaminase active site of the small subunit. The fact that the G359F mutation affects the synchronization of the active sites required for glutamine and MgATP hydrolysis lends further experimental support for the functional existence of the ammonia tunnel in CPS.

Acknowledgments—We thank Dr. W. W. Cleland for carefully reading this manuscript.

REFERENCES

1. Srere, P. A. (1987) *Annu. Rev. Biochem.* **56,** 89–124
2. Anderson, K. S. (1999) *Methods Enzymol.* **308,** 111–145
3. Spivey, H. O., and Ovadi, J. (1999) *Methods* **19,** 306–321
4. Huang, X., Holden, H. M., and Raushel, F. M. (2001) *Annu. Rev. Biochem.* **70,** 149–180
5. Hyde, C. C., Ahmed, S. A., Padlan, E. A., Miles, E. W., and Davies, D. R. (1988) *J. Biol. Chem.* **263**, 17857–17871
6. Thoden, J. B., Holden, H. M., Wesenberg, G., Raushel, F. M., and Rayment, I. (1997) *Biochemistry* **36,** 6305–6316
7. Tesmer, J. J. G., Klem, T. J., Deras, M. L., Davisson, V. J., and Smith, J. L. (1996) *Nat. Struct. Biol.* **3,** 74–86
8. Krahn, J. M., Kim, J. H., Burns, M. R., Parry, R. J., Zalkin, H., and Smith, J. L.

(1997) *Biochemistry* **36,** 11061–11068
9. Larsen, T. M., Boehlein, S. K., Schuster, S. M., Richards, N. G. J., Thoden, J. B., Holden, H. M., and Rayment, I. (1999) *Biochemistry* **38,** 16146–16157
10. Teplyakov, A., Obmolova, G., Badet, B., and Badet-Denisot, M. A. (2001) *J. Mol. Biol.* **313**, 1093–1102
11. Raushel, F. M., Thoden, J. B., Reinhart, G. D., and Holden, H. M. (1998) *Curr. Opin. Chem. Biol.* **5,** 624–632
12. Holden, H. M., Thoden, J. B., and Raushel, F. M. (1998) *Curr. Opin. Struct. Biol.* **8,** 679–685
13. Holden, H. M., Thoden, J. B., and Raushel, F. M. (1999) *Cell Mol. Life Sci.* **56,** 507–522
14. Piette, J., Nyunoya, H., Lusty, C. J., Cunin, R., Weyens, G., Crabeel, M., Charlier, D., Glansdorff, N., and Piérard, A. (1984) *Proc. Natl. Acad. Sci. U. S. A.* **81,** 4134–4138
15. Nyunoya, H., and Lusty, C. J. (1983) *Proc. Natl. Acad. Sci. U. S. A.* **80,** 4629–4633
16. Rubino, S. D., Nyunoya, H., and Lusty, C. J. (1986) *J. Biol. Chem.* **261,** 11320–11327
17. Trotta, P. P., Burt, M. E., Haschemeyer, R. H., and Meister, A. (1971) *Proc. Natl. Acad. Sci. U. S. A.* **68,** 2599–2603
18. Thoden, J. B., Miran, S. G., Phillips, J. C., Howard, A. J., Raushel, F. M., and Holden, H. M. (1998) *Biochemistry* **37,** 8825–8831
19. Thoden, J. B., Raushel F. M., Benning M. M., and Holden, H. M. (1999) *Acta Crystallogr. Sect. D Biol. Crystallogr.* **55**, 8–24
20. Thoden, J. B., Wesenberg, G., Raushel, F. M., and Holden, H. M. (1999) *Biochemistry* **38,** 2347–2357
21. Thoden, J. B, Raushel, F. M., Wesenberg, G., and Holden, H. M. (1999) *J. Biol. Chem.* **274,** 22502–22507
22. Thoden, J. B., Huang, X., Raushel, F. M., and Holden, H. M. (1999) *Biochemistry* **38,** 16158–16166
23. Nicholls, A., Sharp, K. A., and Honig, B. (1991) *Proteins Struct. Funct. Genet.* **11,** 281–296
24. Huang, X., and Raushel, F. M. (2000) *Biochemistry* **39,** 3240–3247
25. Huang, X., and Raushel, F. M. (2000) *J. Biol. Chem.* **275,** 26233–26240
26. Miran, S. G., Chang, S. H., and Raushel, F. M. (1991) *Biochemistry* **30,** 7901–7907
27. Otwinowski, Z., and Minor, W. (1997) *Methods Enzymol.* **276,** 307–326
28. Tronrud, D. E., Ten Eyck, L. F., and Matthews, B. W. (1987) *Acta Crystallogr. Sect. A.* **43,** 489–501
29. Jones, T. A. (1992) in *Molecular Replacement*, (Dodson, E. J., Gover, S., and Wolf, W., eds) pp. 91–105, SERC Daresbury Laboratory, Warrington, England
30. Kleywegt, G. J., and Jones, T. A. (1994) in *From First Map to Final Model* (Bailey, S., Hubbard, R., and Waller, D., eds) pp. 59–66, SERC Daresbury Laboratory, Warrington, England
31. Roussel, A., Fontecilla-Camps, J. C., and Cambillau, C. (1990) *Acta Crystallogr. Sect. A* **46**, C66-C67
32. Huang, X., and Raushel, F. M. (1999) *Biochemistry* **38,** 15909–15914
33. Matthews, B. W. (1996) *FASEB J.* **10,** 35–41
34. Kraulis, P. J. (1991) *J. Appl. Cryst.*, **24,** 946–950